

CD4 Down-regulation by HIV-1 and Simian Immunodeficiency Virus (SIV) Nef Proteins Involves Both Internalization and Intracellular Retention Mechanisms*

Received for publication, August 17, 2004, and in revised form, December 16, 2004
Published, JBC Papers in Press, December 16, 2004, DOI 10.1074/jbc.M409420200

Jeremy J. Rose[‡], Katy Janvier[§], Soundararajulu Chandrasekhar[‡], Rafick P. Sekaly[¶],
Juan S. Bonifacino[§], and Sundararajan Venkatesan^{‡||}

From the [‡]Laboratory of Molecular Microbiology, NIAID and [§]Cell Biology and Metabolism Branch, NICHD, National Institutes of Health, Bethesda, Maryland 20892 and the [¶]Universite de Montreal, Montreal, Quebec H3C 3J7, Canada

Among the pleiotropic effects of Nef proteins of HIV and simian immunodeficiency virus (SIV), down-modulation of cell surface expression of CD4 is a prominent phenotype. It has been presumed that Nef proteins accelerate endocytosis of CD4 by linking the receptor to the AP-2 clathrin adaptor. However, the related AP-1 and AP-3 adaptors have also been shown to interact with Nef, hinting at role(s) for these complexes in the intracellular retention of CD4. By using genetic inhibitors of endocytosis and small interfering RNA-induced knockdown of AP-2, we show that accelerated CD4 endocytosis is not a dominant mechanism of HIV-1 (NL4-3 strain) Nef in epithelial cells, T lymphocyte cell lines, or peripheral blood lymphocytes. Furthermore, we show that both the CD4 recycling from the plasma membrane and the nascent CD4 in transit to the plasma membrane are susceptible to intracellular retention in HIV-1 Nef-expressing cells. In contrast, AP-2-mediated enhanced endocytosis constitutes the predominant mechanism for SIV (MAC-239 strain) Nef-induced down-regulation of human CD4 in human cells.

The cytoplasmic domains of plasma membrane receptors contain sequence determinants that regulate orderly protein sorting during anterograde transport, specify organelle targeting, and determine the intracellular fate of internalized receptors after agonist binding or cell activation (1–3). Animal viruses have evolved several strategies to subvert mechanisms of protein sorting, resulting in aberrant trafficking, intracellular trapping, and degradation of targeted receptors.

Among the viral modulators of receptor expression and trafficking, the 27–32 kDa myristoylated Nef proteins of HIV¹ and

SIV have been most extensively characterized for their ability to down-regulate CD4 and HLA-I receptors (reviewed in Refs. 4–6). These receptors are modulated by different mechanisms and require distinct subdomains of Nef (7–11). Nef reduces the steady-state levels of CD4 apparently by accelerating receptor endocytosis and misdirecting the internalized CD4 to lysosomes for breakdown. A membrane-proximal dileucine motif in the cytoplasmic tail of CD4 is both necessary and sufficient for the HIV-1 Nef-mediated down-regulation (12, 13). Specific interactions of Nef with the components of heterotetrameric adaptor complexes are critical determinants of this process. Mutations at the 2 leucines in the highly conserved (D/E)XXXL(L/I) dileucine motif in the solvent-exposed, C-terminal flexible loop of both HIV and SIV Nef proteins abolish AP-1 and AP-3 adaptor binding and CD4 down-regulation (10, 11, 14, 15). Furthermore, CD4-Nef or CD8-Nef chimeras fusing the ecto- and transmembrane domains of CD4 or CD8 to Nef undergo rapid endocytosis in a dileucine motif-dependent manner (11, 16). SIV Nef has an additional tyrosine-based sorting signal of the type YXXØ, which presumably binds to the AP-2 complex and is implicated in enhancing endocytosis of CD4 (17, 18). From these findings, Nef is presumed to serve as a “connector” between CD4 and the endocytic machinery (6, 16). Such a role would necessitate a physical interaction between Nef and CD4. CD4-Nef complexes have been demonstrated in insect cells overexpressing both proteins (19), in a yeast two-hybrid system (20), and in *in vitro* binding assays with Nef protein and peptides corresponding to the CD4 cytoplasmic domain (21, 22).

The objectives of this study were to inquire whether endocytic enhancement is the sole mechanism of Nef-induced CD4 down-modulation and to elucidate the differences, if any, in the mechanisms of HIV-1 and SIV Nef with respect to recruitment of different adaptor complexes and subunits in the process. Using a yeast three-hybrid assay, we demonstrated recently that (D/E)XXXL(L/I)-type signals from HIV and SIV Nefs interacted in a bipartite manner with the adaptor hemicomplexes, $\gamma\sigma 1$ of AP-1 and $\delta\sigma 3$ of AP-3. The analogous $\alpha\sigma 2$ of AP-2 and $\epsilon\sigma 4$ subunits of AP-4 did not interact with Nef. Interaction of HIV-1 Nef protein with the individual subunits of AP complexes was much weaker or non-existent (15).

We have extended the above studies to show that the loss of CD4 at the cell surface of HIV-1 Nef-expressing cells did not result exclusively from accelerated endocytosis of CD4. Both the recycling CD4 and the nascent receptor in transit to the plasma membrane were susceptible to intracellular retention and degradation in HIV-1 Nef-expressing cells. In contrast, SIV Nef-induced CD4 down-regulation resulted mostly from enhanced endocytosis and was dramatically reversed by genetic

* The costs of publication of this article were defrayed in part by the payment of page charges. This article must therefore be hereby marked “advertisement” in accordance with 18 U.S.C. Section 1734 solely to indicate this fact.

|| To whom correspondence should be addressed: Laboratory of Molecular Biology, Bldg. 10, Rm. 6A05, NIAID, National Institutes of Health, Bethesda, MD, 20892-1576. Tel.: 301-496-6359; Fax: 301-402-4122; E-mail: aradhana@helix.nih.gov or sv1s@nih.gov.

¹ The abbreviations used are: HIV, human immunodeficiency virus; SIV, simian immunodeficiency virus; AP, adaptor protein; APC, allophycocyanin; siRNA, small interfering RNA; PBL, peripheral blood lymphocytes; DMEM, Dulbecco’s modified Eagle’s medium; FCS, fetal calf serum; GFP, green fluorescent protein; EGFP, enhanced GFP; YFP, yellow fluorescent protein; EYFP, enhanced YFP; WT, wild type; FACS, fluorescence-activated cell sorter; PBS, phosphate-buffered saline; MFV, mean fluorescence value; CHAPS, 3-[(3-cholamidopropyl)dimethylammonio]-1-propanesulfonic acid; PE, phosphatidylethanolamine; mAb, monoclonal antibody; CMV, cytomegalovirus; NX, NefXho; Tfn, transferrin; TfnR, Tfn receptor.

inhibitors of endocytosis or small interfering RNA (siRNA)-driven knockdown of AP-2 complexes.

EXPERIMENTAL PROCEDURES

Cells and Viruses—Human T cell lines used in this study included CD4-positive Jurkat cells or the A3.01 derivative of CEM cells and CD4-negative A2.01 cells. These T cell lines and a HeLa CD4 cell line, clone 6C (HT-6C), were obtained from the National Institutes of Health AIDS Research and Reference Reagent Program, Rockville, MD and propagated. The T lymphocytes were propagated in RPMI with 10% fetal calf serum (FCS) and the HeLa CD4 cell line in Dulbecco's modified Eagle's medium (DMEM) with 10% FCS. The HeLa CD4 cells were monitored periodically for the inevitable outgrowth of CD4(-) cells, at which time they were selected on G418 (500 μ g/ml) for two passages. Human T cell lines expressing wild type CD4 (line A2D8), or the tCD4 mutant (line T402), truncated at the 402nd residue and thus lacking the C-terminal domain, were constructed by retroviral transduction of the CD4-negative T cell line A2.01 using a retroviral vector and neomycin selection (23) and maintained in RPMI medium supplemented with 10% fetal bovine serum and periodically selected by G418 (500 μ g/ml) as above. PBLs were isolated from whole blood, buffy coat, or lymphocyte-rich leukopaks provided by the Department of Transfusion Medicine at the National Institutes of Health. Red blood cells were disrupted with ammonium chloride in potassium bicarbonate lysis solution and removed by gentle centrifugation. The final pellet of d0 peripheral blood mononuclear cells was suspended in RPMI with 10% FCS. For T-cell activation, peripheral blood mononuclear cells purified by banding after Ficoll-Hypaque centrifugation were stimulated by CD3 mAb for 36 h in the presence of interleukin-2 (20 IU/ml) in RPMI with 10% FCS, following which they were propagated in medium containing interleukin-2 (24).

All the recombinant vaccinia viruses used in this work had been constructed by homologous recombination at the thymidine kinase locus of the vaccinia virus genome. Plasmid pSC11 was used as the transfer vector. pSC11 contains the vaccinia virus 7.5K promoter for the expression of foreign genes and also had an *Escherichia coli lac-Z* gene linked to the vaccinia virus 11k promoter. The following recombinant vaccinia viruses were used: 1) for negative control, the recombinant vaccinia virus (vSC8) encoding the *E. coli lac-Z* (25); 2) vvNef that was isogenic with vSC8 except for the *Nef* gene linked to the 7.5K promoter (26); 3) vvCD4 (vCB-7) expressing WT full-length human CD4 (27); 4) vvtCD4 (vCB-2) expressing CD4 truncated at residue 402 (and modified by the addition at the C terminus of a Leu-Ileu-Asn sequence during DNA cloning) and thus lacking the cytoplasmic domain (28); 5) vvgp160 (vPE16) expressing the HIV-1 envelope glycoprotein, gp160 (29, 30); and 6) vvCD46, expressing the human CD46 protein (31). Cloned virus stocks were plaque-purified thrice on CV-1 cells, propagated in HeLa S3 suspension cells, and purified by banding on sucrose gradients by ultracentrifugation (29, 30). For expression studies, cells were infected at a multiplicity of infection of 5 or 10 plaque-forming units/cell unless indicated otherwise.

Recombinant DNA Constructs—The original Nef expression plasmid, pCMV-Nef, has been described (32). For expression in mammalian cells, wild type or mutant Nef cDNAs were PCR-amplified from the respective HIV and SIV proviruses or other recombinant plasmids and cloned into EcoRI-SalI sites of pCI-neo vector (Promega, Madison, WI). CMV promoter-linked CD4 and CD8 plasmids were obtained from the National Institutes of Health AIDS Research and Reference Reagent Program, Rockville MD. CD4 was mutated by a two-step PCR mutagenesis protocol (33) to exchange the codons for 2 leucines at 438–439 to alanines and cloned into the pCI-neo vector to generate LL/AA CD4. Dominant-negative Eps15 deletion mutant fused N-terminally to GFP (GFP-Eps15 Δ 95/295) was obtained from Alexandre Benmerah at INSERM, Paris, France (34). GFP-tagged WT dynamin and the K44A dominant-negative dynamin mutant (35) were from Julie Donaldson at NICHD, National Institutes of Health, Bethesda, MD. EYFP-tagged Rab5 and Rab5-S34N have been described (24).

Antibodies—The following mouse monoclonal antibodies were obtained: 1) against α , γ , δ , and ϵ -adaptins, unconjugated or dye-conjugated CD71 (transferrin receptor, TfnR), and unconjugated CD46 (BD Transduction and Pharmingen Laboratories) and 2) unconjugated, Alexa Fluor 488-, PE-, or APC-conjugated CD4 and CD8 mAbs (Caltag Laboratories, Burlingame, CA). The following polyclonal antibodies were also used: 1) against the σ 3 subunit of AP-3 adaptor (36) and 2) against TfnR (Zymed Laboratories Inc., South San Francisco, CA). Monoclonal antibody (TW 2.3) against the vaccinia virus E3L gene product (37) was a gift from Jonathan Yewdell, NIAID, National Insti-

tutes of Health. Rabbit antiserum against HIV-1 gp160 protein was a gift of Ronald Willey, NIAID, National Institutes of Health. Secondary antibodies to mouse, rabbit, goat, and sheep IgG conjugated to Alexa Fluor 488, 568, or 647 dyes were from Molecular Probes Inc. (Eugene, OR).

Cell Culture and Transfections—HeLa cells, cultured in DMEM supplemented with 10% FCS (v/v), were transfected using the Lipofectamine Plus reagent (Invitrogen) according to the manufacturer's instructions. PBLs were isolated from whole blood, buffy coat, or lymphocyte-rich leukopaks provided by the Department of Transfusion Medicine at the Clinical Center, National Institutes of Health, as described (24). CD4+ T cells were enriched by negative selection using magnetic bead technology (Miltenyi Biotec Inc., Auburn, CA). PBLs and T cell lines were transfected using an Amaxa Biosystems electroporator with the recommended reagents (AMAXA Inc., Gaithersburg, MD).

Flow Cytometry—General protocols of flow cytometry using HeLa cell transfectants, primary T cells, and lines have been described before (24). In all transfections, plasmids encoding EGFP or CD8 were included to normalize for transfection efficiency. For detection of internal antigens, the cells were permeabilized with 0.1% saponin treatment and fixed in 4% paraformaldehyde prior to antibody staining in the presence of 0.1% saponin. Vaccinia virus infection was monitored by FACS analysis of cells permeabilized by saponin, using a monoclonal antibody (TW 2.3) against the vaccinia virus E3L gene product (37). At 4 h after vaccinia virus infection, 40–60% of cells scored positively with this antibody.

CD4 Endocytosis and Recycling—CD4 endocytic kinetics was determined by flow cytometry assay essentially as described previously (38, 39). HeLa cells were co-transfected with WT or mutated CD4 along with WT Nef or the NefXho (NX) Nef deletion mutant. Alternatively, Jurkat cells were transfected with Nef or NX plasmid. In all transfections, CD8 plasmid was included to enable gating of transfected cells. At 30 h after transfection, cells were reacted with PE-conjugated Leu3A mAb for 30 min on ice in DMEM or RPMI 1640 (for Jurkat cells) containing 0.5% bovine serum albumin. An aliquot of cells was co-stained at 0–4 °C with CD8 APC to determine the transfection efficiency and CD4 PE to quantify the CD4 receptor density at the cell surface. The bulk of the cells that had been stained with CD4 PE only were rinsed thrice with RPMI containing 0.5% bovine serum albumin at 2–4 °C to remove the excess unbound antibody and incubated at 37 °C. At the indicated times, dual 50- μ l aliquots were diluted with 5–10 volumes of RPMI at neutral or acid pH (pH 2 for HeLa cells, pH 3 for Jurkat cells) and incubated for 45 s at 2–4 °C. After rinsing with neutral pH RPMI, cells were fixed in 4% paraformaldehyde in PBS for 10 min at 2–4 °C, rinsed with PBS, and counterstained with CD8-APC and processed for flow cytometry. Mean fluorescence values (MFVs) for CD4 were calculated for cells gated for CD8 expression. To calculate the fraction of CD4 internalization at each time point, $[F(\text{int})_{\text{ti}}]$, the CD4 MFV at zero time acid wash $[MFV(\text{pH } 2)_{\text{t0}}]$ was subtracted from the MFVs for each time point $[MFV(\text{pH } 2)_{\text{ti}}]$ times, and the resulting value for each time point was divided by the total MFV (neutral pH wash) $[MFV(\text{pH } 7.4)_{\text{ti}}]$ as indicated by the equation below.

$$F(\text{int})_{\text{ti}} = \frac{[MFV(\text{pH } 2)_{\text{ti}} - MFV(\text{pH } 2)_{\text{t0}}]}{MFV(\text{pH } 7.4)_{\text{ti}}} \times 100 \quad (\text{Eq. 1})$$

For microscopic visualization of CD4 endocytosis, fluorescent antibody was fed to living cells together with fluorescent transferrin as a monitor for clathrin-dependent endocytosis of TfnR. HeLa cells transiently expressing CD4, WT Nef, or Nef-Xho mutant and GFP- or YFP-tagged dominant-negative inhibitors of endocytosis were used. Cells on coverslips at 50% confluence were starved for 30 min at 37 °C in DMEM without serum. They were then incubated at 37 °C for 30 min in 200 μ l of DMEM (with 0.5% bovine serum albumin) with Alexa Fluor 568-conjugated Tfn (50 μ g/ml) and APC-labeled CD4 mAb (10 μ l of mAbs or 1–2 μ g of equivalent). Cells were rinsed thrice with PBS, fixed with paraformaldehyde, rinsed and mounted in Fluoromount-G (Southern Biotechnology Associates, Birmingham, AL). In some experiments (indicated in the relevant figure legends), cell surface bound antibody was stripped by treatment for 1–2 min with 0.5% acetic acid in 500 mM NaCl after the first rinse before fixation.

CD4 recycling was calculated as described (39) with slight modifications. HeLa cell transfectants were labeled with PE-conjugated CD4 mAb as for endocytosis studies, incubated at 37 °C for 30 min to maximize antibody internalization, rinsed, and suspended in 5 volumes of RPMI at pH 2 at 4 °C for 2 min. Cells were then transferred to neutral buffer, and a time 0 aliquot was collected, fixed, and counterstained with CD8-APC and analyzed by FACS. The remaining cells were

warmed to 37 °C for the indicated times, placed in timed aliquots, washed in cold acid, fixed, and counterstained for CD8. CD4 MFVs in the CD8 gated population was determined by FACS analysis. The percentage of recycled CD4 was determined by dividing the MFVs during the rewarming period by the acid-resistant MFV before rewarming.

Yeast Culture, Transformation, and Two- and Three-hybrid Assays—Two-hybrid genetic analysis between various Nefs and the adaptor subunits was carried out as described before (15). The *Saccharomyces cerevisiae* strain HF7c (Clontech) was maintained on dropout agar plates lacking methionine. Transformation was performed by the lithium acetate procedure as described in the instructions for the MATCH-MAKER two-hybrid kit (Clontech). HF7c transformants were selected by spreading on plates lacking leucine, tryptophan, and methionine. For colony growth essays, HF7c transformants were dotted on plates lacking leucine, tryptophan, methionine, and histidine complemented with 3 mM 3-aminotriazole (Sigma) and allowed to grow at 30 °C for 3–5 days.

Metabolic Labeling and Immunoprecipitation—For metabolic labeling experiments, transfected or virus-infected HeLa cells or T cells (10^6 – 10^7) were rinsed thrice with PBS and incubated in methionine and cysteine-free DMEM containing 1% dialyzed FCS (0.2 ml/sample) for 10 min. For steady-state labeling, cells were incubated for 1 h by the addition of ^{35}S -labeled Trans-label (ICN Corp) to 1 mCi/ml. For measuring the kinetics of protein biosynthesis, 2×10^7 cells were labeled for 15 min in 500 μl of labeling medium (1 mCi/ml). At the end of the labeling, the cells were diluted with 10 volumes of complete RPMI medium. Aliquots were removed immediately after labeling and at the indicated periods during the chase (from 0 to 12 h). The cells were rinsed twice in PBS and processed for SDS-PAGE analysis. The cells were disrupted by three cycles of freeze-thawing (thawing to 37 °C for 1–2 min to disrupt rafts) in 500 μl of extraction buffer containing 0.05 M Tris-HCl, pH 7.4, 100 mM NaCl, 0.25% Nonidet P-40 (or CHAPS), 0.25% Triton X-100, and one tablet of protease inhibitor mix (Roche Applied Science) followed by extraction at 4 °C for 1 h. The extracts were centrifuged at $10,000 \times g$ for 10 min, and supernatants were used for immunoprecipitation. The supernatants were precleared by incubation for 1 h at 4 °C with 30 μl of immobilized protein G agarose beads (Pierce) coated with preimmune rabbit or mouse sera. Labeled proteins were immunoprecipitated for 3 h at 4 °C with protein G agarose beads prebound to the corresponding anti-rabbit polyclonal or anti-mouse monoclonal antibodies. Following specific antibody binding, the beads were collected by centrifugation and washed five times with 10–20 volumes of extraction buffer lacking protease inhibitors, and the labeled proteins were eluted by boiling in 50 μl of a buffer containing Tris-HCl, pH 7.4, 100 mM NaCl, 50 mM dithiothreitol, 2% SDS, glycerol (10% v/v), and bromophenol blue (0.1% w/v). The radiolabeled proteins were resolved by SDS-PAGE and visualized by phosphorimaging and quantified.

Immunofluorescence Microscopy—Twenty-four hours after transfection, HeLa cells grown on glass coverslips were stained for immunofluorescence microscopy. Cells were fixed in 4% paraformaldehyde in PBS and permeabilized for 10 min with 0.1% (w/v) Triton X-100 in PBS. After permeabilization, the cells were blocked for 30 min with 1% normal goat serum in PBS and incubated for 30 min at room temperature with the primary antibody, washed with PBS, and then incubated for 30 min with the secondary antibody. The different combinations of 1° and 2° antibodies and GFP or GFP fusion proteins are indicated in the respective figure legends. The coverslips were washed and mounted on slides. Images were collected on a Leica TCS-NT/SP confocal microscope (Leica Microsystems, Exton, PA) using a $\times 63$ or $\times 100$ oil immersion objective NA 1.32 and digital zoom up to $\times 5$. Fluorochromes were excited using an argon laser at 488 nm for Alexa Fluor 488 or fluorescein isothiocyanate, a krypton laser at 568 nm for Alexa Fluor 568 or Texas Red, and a helium/neon laser at 633 nm for APC. Fluorescent emission from Alexa Fluor 350 dye was visualized by excitation with a UV laser. Detector slits were configured to minimize any cross-talk between the channels, or the channels were collected separately and later superimposed. Differential interference contrast images were collected simultaneously with the fluorescence images using the transmitted light detector. Eight or more fields were examined per coverslip, and each experimental condition was repeated as indicated in the respective figure legends.

RNA-mediated Interference—RNA-mediated interference of $\mu 2$ adaptor subunit or vps35 was performed using an siRNA duplex with the following sequence: $\mu 2$, 5'AAGUGAUGCCUUUCGGUCA-3' starting at the 30th codon (86th nucleotide in the open reading frame); $\mu 3$, 5'AAGGAGAACAGUUCUUGCGGC-3'; and vps35, 5'AAGUCCAGU-

CAUUCCAAUG-3' starting at the 24th codon (70th nucleotide in the open reading frame). HeLa cells were transfected twice at 72-h intervals with 200 nM of the siRNAs, using Oligofectamine (Invitrogen). After 144 h of siRNA treatment, the cells were transfected as described above for expression of Nef, CD4, and CD8. Human T cell lines and PBLs were electroporated once with 100 nM siRNA using the Amaxa system. The cells were rested for 24–36 h before electroporating with an additional 100 nM siRNA and expression plasmids as indicated in the relevant figure legends.

RESULTS

HIV-1 Nef Delayed the Cell Surface Expression and Reduced the Cell Surface Density of de novo Synthesized CD4—Initially, we examined the kinetics of transport to the plasma membrane of *de novo* synthesized CD4 in the context of Nef expression. A2.01 (CD4-negative) T lymphocytes were co-infected with recombinant vaccinia viruses encoding WT CD4 (vCB-7) and NL4-3 HIV-1 Nef allele (vvNef) or a control virus (vSC8). Following 30 min of virus adsorption, cells were sampled at periodic intervals and examined by flow cytometry. Both sets of infected cells displayed similar levels of endogenous CD7 expression (not shown) that was used to monitor potential non-specific effects of vaccinia virus infection on cellular receptor expression. The progress of vaccinia infection was monitored by flow cytometry of fixed and permeabilized cells stained with mAb against E3L protein, an early vaccinia virus gene product. Substantial E3L expression was observed in >60% of cells (not shown) in both sets of co-infections. vCB-7/vSC8-infected cells displayed significant cell surface CD4 expression by 2–3 h after infection, and by 6 h after infection, >60% of cells were positive for CD4 expression (Fig. 1, top row). In contrast, vCB-7/vvNef-infected cultures lagged behind the vCB-7/vSC8 counterparts in the acquisition of CD4 surface staining and expressed significantly less CD4 at the cell surface. At 6 h after infection, only 20% or less of the vCB-7/vvNef-infected cells were positive for CD4 expression (Fig. 1A, bottom row). Nef expression was detected in vvNef cells (by immunoblotting) within 15–30 min after adsorption and continued unabated (not shown). When a recombinant vaccinia virus expressing tailless/truncated CD4 (tCD4) was used in place of WT CD4, Nef did not cause measurable difference in tCD4 expression (not shown). Thus, during simultaneous expression in T cells, Nef significantly delayed the cell surface expression and reduced the overall plasma membrane density of co-expressed CD4.

HIV-1 Nef Accelerated the Metabolic Turnover of Co-expressed CD4 in Recombinant Vaccinia Virus-infected T Cells and in Epithelial Cell Transfectants—We then inquired whether the delayed cell surface appearance of CD4 in HIV-1 Nef (+) cells reflected aberrant metabolic turnover of *de novo* synthesized receptor. A2.01 cells were infected with recombinant vaccinia viruses for WT CD4 (vCB-7) and vvNef or control vaccinia (vSC8). At the peak of early vaccinia gene expression (about 2 h after infection), the turnover rates of *de novo* synthesized CD4 and other recombinant proteins were evaluated in metabolic labeling experiments. As shown in Fig. 1B, there was a marked enhancement in the turnover rate of labeled CD4, with a $t_{1/2}$ of about ~3 h. In contrast, CD4 in vSC8-infected cells remained stable throughout the chase period. The Nef-induced phenotype was specific for WT CD4. Nef had no effect on the turnover of tCD4 lacking the cytoplasmic tail.

Although HIV-1 Nef induced significant increase in the metabolic turnover of WT CD4, it had no effect on the unrelated CD46 expressed from a separate recombinant, vvCD46, that was included in the vSC8/vCB7 or vvNef/vCB7 co-infections (Fig. 1C, left). When a HIV-1 gp160 recombinant, vPE16, was included in a similar triple infection, Nef expression actually induced a slight stimulation of gp160 labeling but no significant change in the turnover rate or processing of gp160 to

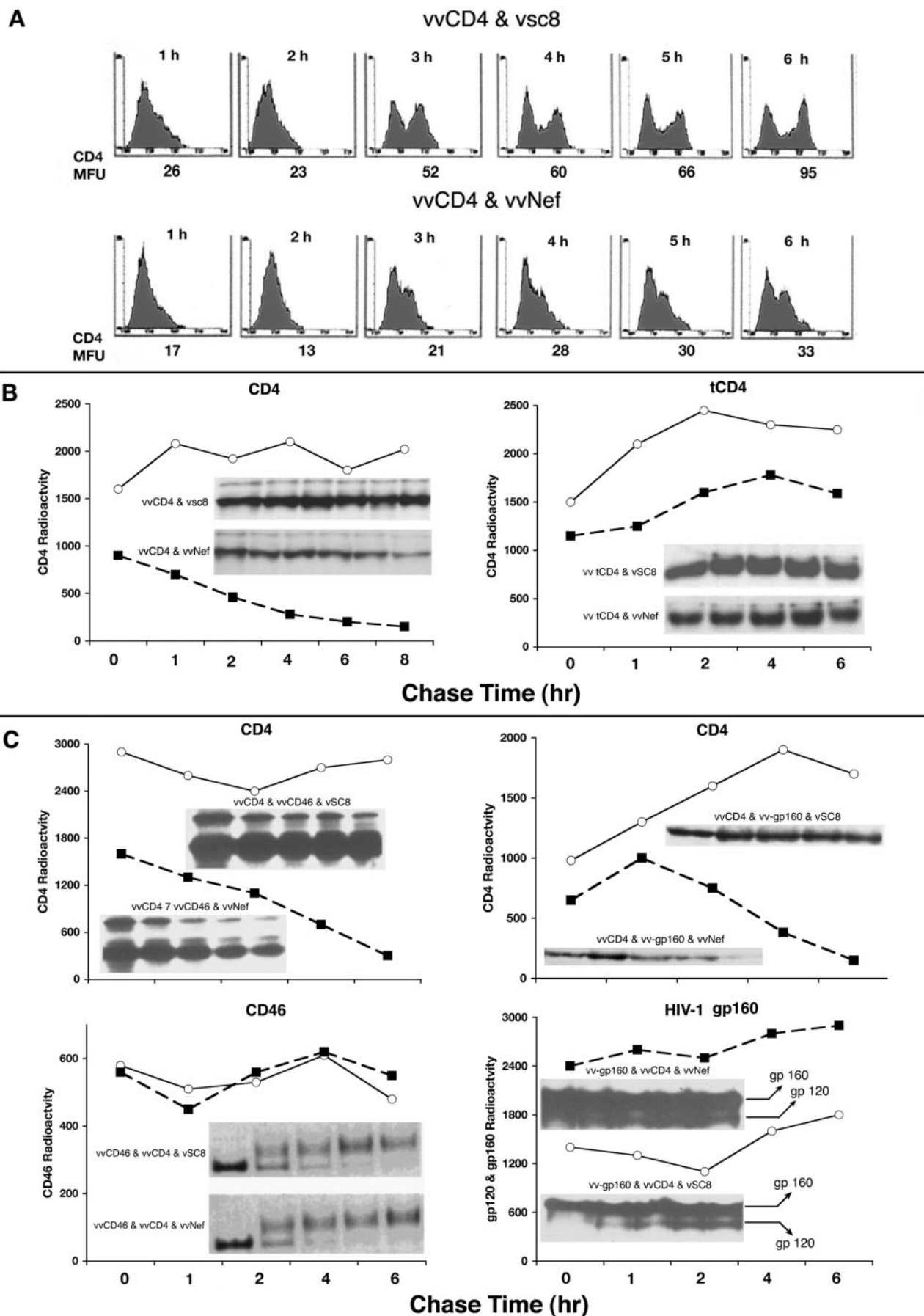
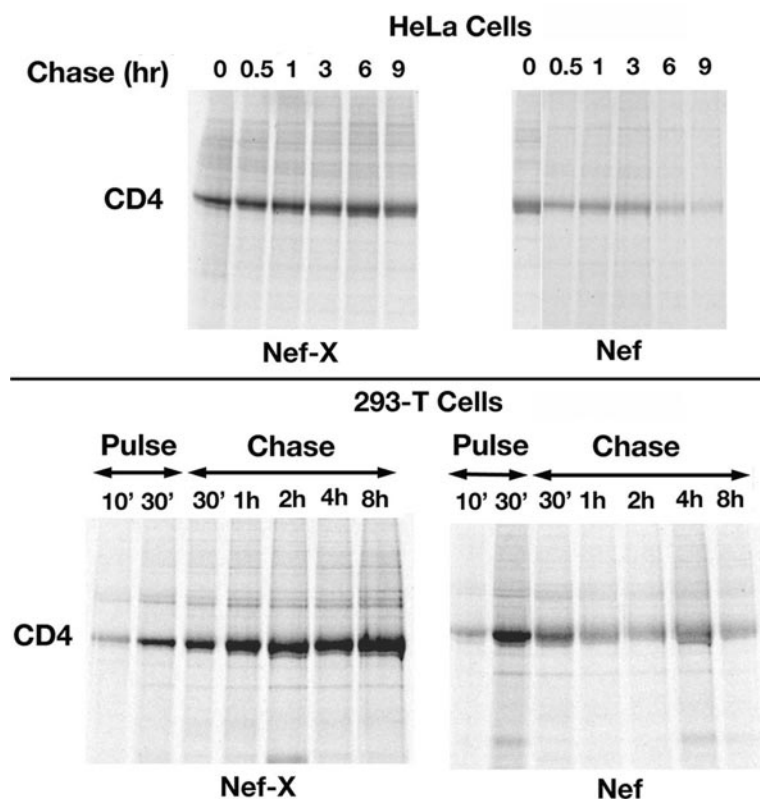


FIG. 1. In simultaneous infections of CD4(-) T cells with recombinant vaccinia viruses expressing Nef and CD4, Nef delayed the cell surface expression and reduced the cell surface density of *de novo* synthesized CD4. A, CD4-negative A2.01 T cell lines were infected with a recombinant vaccinia virus encoding CD4 (vCB-7) and vSC8 control recombinant (*top*) or vvNef (*bottom*) at a total multiplicity of infection

FIG. 2. Nef-induced rapid metabolic turnover of co-expressed in epithelial cells. 2×10^7 HeLa (*top*) or 293-T cells (*bottom*) were co-transfected with CMV-CD4 and CMV-Nef or CMV-NefXho at a molar ratio of 1:1.5. CMV-CD8 (at 0.5 molar ratio) was included in each sample to monitor transfection efficiencies. At 36 h after transfection, cells were evaluated for CD4 and CD8 expression by flow cytometry. Metabolic turnover of CD4 was analyzed by pulse-chase labeling as described under "Experimental Procedures." CD4 levels were determined by quantitative immunoprecipitation and phosphorimaging after adjusting the respective lysates for constant CD8 expression. Fluorographic gel profiles and CD4 metabolic turnover plots representing two each of HeLa cell and 293-T cell transfections are shown.



gp120 (Fig. 1C, *right*). When CD4 and gp160 are co-expressed, gp160 egress out of the endoplasmic reticulum might be hindered, resulting in the degradation of both CD4 and gp160 (40–42). The enhanced gp160 labeling probably reflected the reduced CD4 levels in the CD4/Nef co-infections, which might have spared the nascent gp160.

We confirmed the above results in HeLa and 293-T cells transiently expressing CD4 and HIV-1 Nef. HeLa and 293-T cells were co-transfected with CMV promoter-linked CD4, CD8, HIV-1 Nef, or Nef-Xho (null Nef) plasmids. Nef or Nef-Xho transfectants were adjusted to reflect equivalent CD8 (+) cells and were subjected to pulse-chase labeling. Nef expression dramatically enhanced the metabolic turnover of nascent CD4 even during the first 30 min of metabolic chase, with a $t_{1/2}$ of about 30 min in 293-T cells and ~ 1 h in HeLa cells (Fig. 2). Thus, in both epithelial cells and T lymphocytes, HIV-1 Nef induced a rapid decay of nascent CD4, which might be occurring even during the receptor transport to the plasma membrane.

SIV Nef Was More Efficient than HIV-1 Nef in Accelerating CD4 Endocytosis in Both HeLa Cells and Jurkat Lymphocytes—Next, we inquired whether enhanced CD4 endocytosis represented a significant mechanism for the loss of cell surface CD4 induced by HIV-1 and SIV Nef proteins. HeLa cells were transfected with CD4, CD8, and HIV-1 or SIV Nef or a null

plasmid (NX). In parallel transfections, a CD4 mutant, LL/AA CD4, exchanging the dileucine codons at 413–414 of mature CD4 to dialanines, was substituted for WT CD4. HIV-1 Nef induced a 3-fold reduction of WT CD4 at the plasma membrane but was without effect on the LL/AA mutant (Fig. 3A, *bottom*). We evaluated the endocytic rates for WT or LL/AA CD4 by determining the intracellular delivery of antibody bound to CD4 at the cell surface. The internalized fraction of fluorescent (PE) antibody bound to CD4 at the cell surface was calculated at different times after initial antibody binding. As expected, WT CD4 underwent brisk endocytosis in HeLa cells that lack the tyrosine kinase *p56 lck* which anchors CD4 to the plasma membrane in T cells (43). In accord with other reports (12, 13), LL/AA CD4 did not undergo constitutive endocytosis (Fig. 3A, *top plot*). HIV-1 Nef expression, which induced 3-fold or higher reduction in the CD4 levels at the plasma membrane (Fig. 3A, *lower panel*), increased the endocytic rate of the residual (3-fold reduced) CD4 at the cell surface only slightly (Fig. 3A, *top panel*). In contrast, SIV Nef induced a more significant endocytosis (2-fold higher initial rates) of residual cell surface CD4, resulting in internalization of $>75\%$ of the receptor from the cell surface before 60 min (Fig. 3B). As shown for HIV-1 Nef, SIV Nef also failed to down-regulate or enhance endocytosis of LL/AA CD4 (Fig. 3B).

Since HIV-1 Nef did not significantly accelerate CD4 endo-

of 10 plaque-forming units/cell. FACS profiles of vaccinia virus E3L expression were used to verify that equivalent levels of vaccinia infection had occurred. The time course of CD4 expression at the cell surface is given by the FACS histogram profile, with the time points denoted above and the average CD4 MFVs denoted below each plot. CD4 MFV values were calculated for cell populations gated for E3L expression. *B*, HIV-1 Nef enhanced the metabolic turnover of CD4 but not of tCD4 mutant lacking the C-terminal domain. Co-infections were set up as in *A*, with the difference that in separate infections with vSC8 or vvNef, a recombinant encoding tCD4 (vCB-2) was substituted for vCB7 (WT CD4). *C*, Nef expression does not significantly alter the metabolic turnover of HIV-1 gp160 or CD46. Co-infections with the respective combination of vaccinia viruses were set up as in *A*, with the difference that co-infections included vvNef or vSC8 and vCB-7 with a recombinant for CD46 (vvCD46) or HIV-1 gp 160 (vPE-16). Vaccinia virus E3L expression was analyzed by flow cytometry of infected cells or immunoprecipitation on a fraction of cell extracts. Extracts were adjusted to equivalent E3L expression and processed for immunoprecipitating the indicated proteins as described under "Experimental Procedures." Representative plots of two experiments (for tCD4 alone and CD46 or HIV gp160 with WT CD4) and three (for WT CD4 alone) are shown.

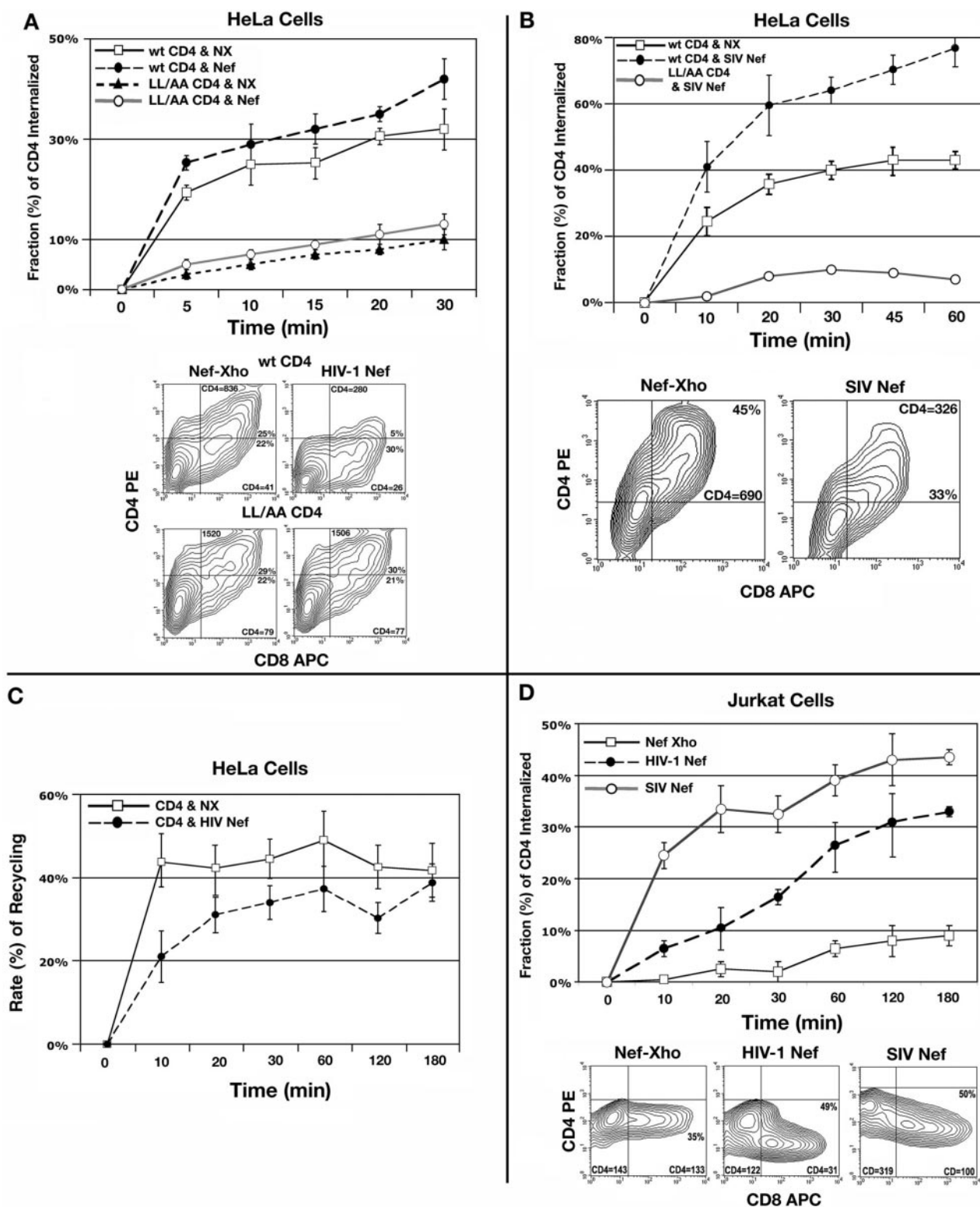


FIG. 3. Unlike SIV Nef, HIV-1 Nef does not significantly enhance the intrinsic endocytic potential of CD4 in HeLa cells or Jurkat lymphocytes, but HIV-1 Nef delays the recycling of internalized CD4. *A*, endocytic rate profiles of WT CD4 or LL/AA mutant in HeLa cell transfectants in the context of HIV-1 Nef or null (NX) expression are shown at the top. CD8 was co-transfected for normalizing transfection efficiency and for gating on the transfected population. PE or APC-conjugated CD4 and CD8 mAbs were used for quantitative flow cytometry. For each time point, the internalized fraction of cell surface CD4 was calculated for each transfection as described under "Experimental Procedures," and the average results from four experiments are plotted with error bars. The bivariate FACS contour diagrams below the plots illustrate the representative steady-state CD4/CD8 expression profiles for the various transfections. Note that HIV-1 Nef induced a 3-fold reduction in the WT CD4 levels at the plasma membrane but was without effect on LL/AA CD4 mutant. *B*, endocytic rate plots (average of four experiments) of WT and LL/AA CD4 in HeLa cells expressing SIV-Nef with a representative FACS contour profile of CD4 and CD8 expression as in *A*. *C*, CD4 recycling rates in HeLa transfectants were measured by the recovery of internalized CD4 mAb in an antibody feeding experiment described under "Experimental Procedures." *D*, rate plots of CD4 endocytosis in Jurkat cells transfected with null, HIV-1, or SIV Nef plasmids. Unlike the HeLa cell experiments measuring the endocytosis of plasmid-expressed CD4, the plots in this panel show internalized fractions of native (endogenous) CD4. Endocytosis was monitored over a 3-h period. HIV-1 and SIV Nef induced a 3–4-fold reduction of cell surface CD4 in Jurkat cells, as illustrated by the representative FACS contour diagrams of CD4 and CD8 expression below the graph.

TABLE I
Effects of HIV-1 or SIV Nef on CD4 Endocytosis in HeLa Cells and Jurkat lymphocytes

Averaged results from six or eight experiments for HIV-1 Nef and CD4 in Jurkat or HeLa cells and six or five experiments for SIV Nef. NA, not applicable.

	Endocytosis rate ^a				
	(-) Nef	(+) HIV-1 Nef	+H-Nef/-Nef	(+)SIV Nef	+S-Nef/-Nef
	%/min	%/min		%/min	
HeLa: wt CD4 for H-Nef	4 ± 0.25	4.8 ± 0.75	1.2		
HeLa: AA CD4 for H-Nef	0.4 ± 0.05	0.5 ± 0.09	NA		
HeLa: wt CD4 for S-Nef	4.1 ± 0.3			8.2 ± 0.55	2
HeLa: AA CD4 for S-Nef	0.2 ± 0.05			0.1 ± 0.02	NA
Jurkat: H or S Nef	0.15 ± 0.02	0.5 ± 0.1	3.33	2.5 ± 0.2	16.66

^a Endocytosis rates were normally calculated over the first 5 min after warming to 37°C for HIV-1 Nef versus NX and over 10 min for SIV Nef versus NX. AA-CD4 refers to the 438LL/AA439 CD4 mutant. Endocytic rates were calculated over the initial 10 min for Jurkat cells. In Jurkat cells, endocytosis was measured for the endogenous CD4 and in HeLa cells results are for the plasmid expressed CD4. Experimental details are given under "Experimental Procedures" and in the legend for Fig. 3.

cytosis, we inquired whether HIV-1 Nef modulated the recycling kinetics of internalized CD4 in HeLa cells. PE-conjugated CD4 antibody bound to the cell surface was allowed to internalize over a 45-min period. After treatment at pH 2 to remove the residual antibody at the cell surface, cells were incubated to allow the antibody to recycle to the cell surface. Previous studies have shown that in HeLa cells and T lymphocytes lacking *p56 lck*, internalized CD4 is promptly returned to the cell surface via recycling endosomes, without encountering the low pH environment of late endosomes or lysosomes (12, 13). HIV-1 Nef expression reduced significantly the initial rate of CD4 recycling during the first 10 min and induced a modest reduction in the total amount recycled over a 1–2-h period (Fig. 3C). The loss of CD4 recycling in Nef (+) cells might reflect reduced recycling rates or aberrant trafficking routing the internalized receptor to lysosomes, where antibody dissociation or CD4 degradation might occur.

It was likely that any potential enhancement of CD4 endocytosis by Nef might be masked by the brisk constitutive recycling kinetics of CD4 in epithelial cells (13, 39). Therefore, we examined CD4 endocytic kinetics in Jurkat T lymphocytes. As expected (44), there was very little, if any, constitutive internalization of CD4 in these cells that have *p56 lck* anchoring CD4 to the plasma membrane (Fig. 3D). Interestingly, both HIV-1 and SIV Nef accelerated CD4 endocytosis in Jurkat cells, although SIV Nef was significantly better in augmenting CD4 internalization over the first 10–20 min. Table I summarizes the effects of HIV-1 or SIV Nef on the endocytic rates of CD4 in HeLa cells or Jurkat lymphocytes. Although HIV-1 Nef did not significantly enhance (~20% increase) the intrinsic endocytic potential of CD4 in HeLa cells, SIV Nef was more potent, enhancing CD4 internalization 2-fold. With Jurkat lymphocytes, there was a significant difference in the magnitude of CD4 endocytosis induced by HIV-1 Nef (3.7-fold) versus SIV Nef (17-fold). Taken together, the above results highlighted mechanistic differences between HIV-1 and SIV Nef for CD4 down-regulation, with the endocytic enhancement being the preferred strategy used by SIV Nef.

HIV-1 Nef-induced Loss and Degradation of Presynthesized CD4 at the Plasma Membrane Was Blocked by Pretreatment with Lysosomotropic Agents—Nef-induced CD4 loss at the plasma membrane might reflect intracellular sequestration or degradation of the receptor. Although HIV-1 and SIV Nef induced a 6-fold (±7%) or a 3.5-fold (±10%) loss of CD4 at the cell surface, the total cellular CD4 was reduced by 50% (±8%). Neither Nef protein had any demonstrable effect on the co-expressed CD8 (Fig. 4A). To focus on the Nef effect on CD4 at the cell surface, we examined the effect of Nef in the absence of concurrent *de novo* CD4 synthesis. Toward this goal, we evaluated CD4 density on CD4 (+) human T cells or a HeLa CD4 cell line expressing HIV-1 Nef from the recombinant vaccinia

virus, vvNef. Since vaccinia virus shuts off host cell synthesis within minutes of virus entry, this approach allowed us to determine the metabolic turnover of presynthesized CD4 in the context of Nef expression. Human T lymphocytes expressing WT CD4 were infected with vvNef or vSVC8 or left untreated. As illustrated in Fig. 4B, there was a 3.5-fold (±8%) loss of plasma membrane-associated CD4 in vvNef-infected cells. There was a proportionate decrease in total cellular CD4 (the immunoblot under the FACS histogram). Under the same conditions, Nef expression had no effect on the expression of endogenous CD2 or CD7 receptors in the same cell line (not shown). More pointedly, Nef expression did not alter the plasma membrane density of a CD4 mutant (tCD4), lacking the C-terminal tail and therefore being intrinsically incapable of being endocytosed (Fig. 4B, bottom).

CD4 and other receptors that are internalized constitutively and/or after ligand binding are either recycled from the early endosomes or routed to the late endosomes and lysosomes, where they are degraded by acidic proteases. This proteolysis can be prevented by treatment of cells with weak bases or protease inhibitors. Therefore, we inquired whether weak bases such as NH₄Cl or chloroquine would reverse the effect of Nef on presynthesized CD4 at the cell surface. As represented by the histograms in Fig. 4C, pretreatment with chloroquine completely reversed the 3-fold down-regulation of presynthesized endogenous CD4 in vvNef-infected T lymphocytes. Likewise, NH₄Cl pretreatment efficiently blocked the net loss of CD4 at the cell surface of vvNef-infected HeLa CD4 cells (Fig. 4D). Thus, aberrant trafficking of internalized CD4 to the lysosomes constituted an important mechanism of HIV-1 Nef-induced CD4 down-modulation. However, this mechanism could only be unraveled in the absence of ongoing CD4 synthesis.

Dominant-negative Inhibitors of Endocytosis Caused a Modest Inhibition of CD4 Down-regulation by HIV-1 Nef—We next assessed the contribution of endocytosis to the HIV-1 Nef-induced loss of concurrently synthesized CD4. We evaluated the effect of Nef on CD4 in transient transfectants under conditions that inhibited endocytic trafficking. To block discrete steps in endocytic trafficking, we used GFP- or YFP-tagged dominant-negative inhibitor mutants of: dynamin, a known effector of vesicular traffic from the plasma membrane (45); Eps15, a critical regulator of clathrin-coated vesicle assembly (34, 46); and Rab5, required for clathrin-coated vesicle fusion with the early endosomes (47).

HeLa cells, Jurkat lymphocytes, or CD4 (+) PBLs were co-transfected GFP- or YFP-tagged fusion proteins listed above with HIV-1 Nef or a null Nef mutant, NX, and a CD4 plasmid for HeLa cells. CD4 expression was measured for GFP-gated transfectants by flow cytometry. First, we compared the effect of GFP versus various tagged fusion proteins on the steady-

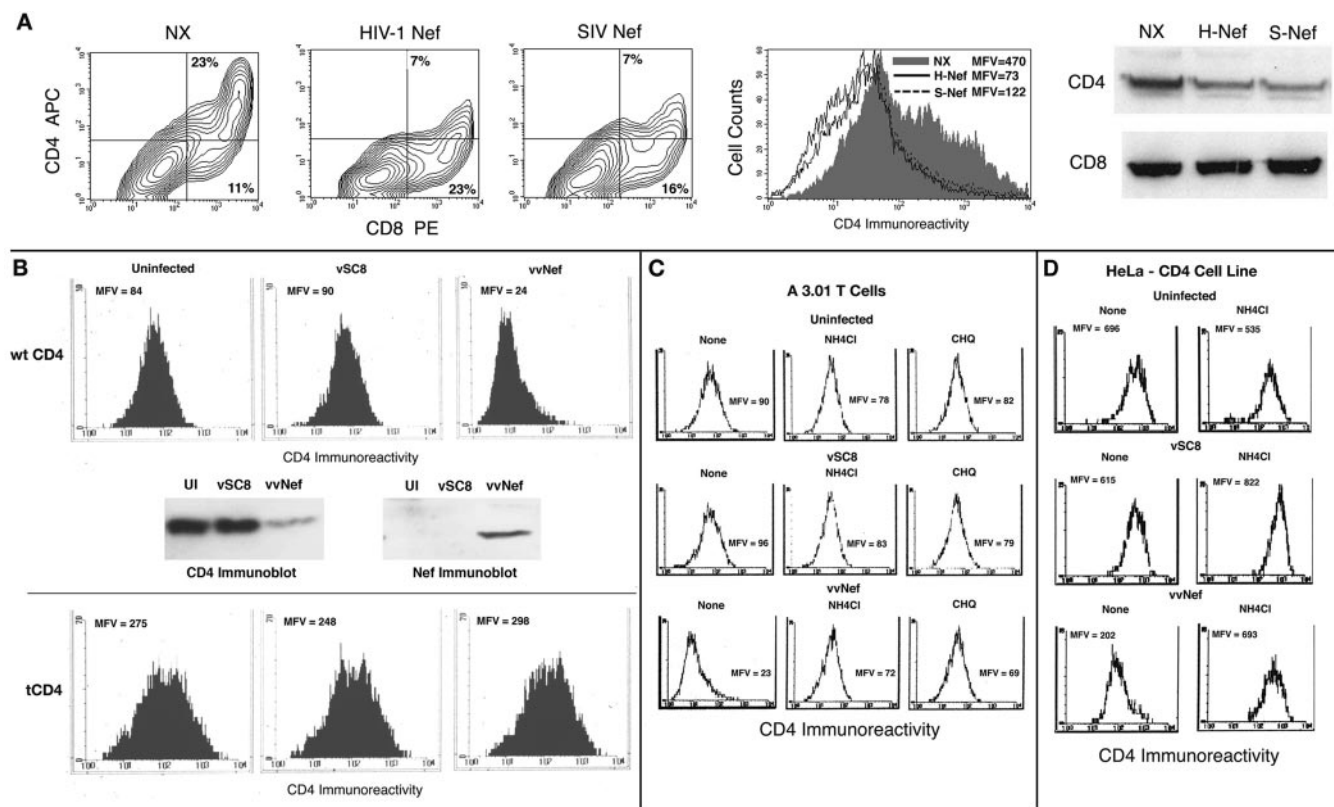


FIG. 4. Both HIV-1 and SIV Nefs induce CD4 degradation, probably in the lysosomes. *A*, under steady-state conditions, both HIV-1 and SIV Nef induced a marked loss of CD4 at the plasma membrane and a modest loss of total cellular CD4. Bivariate contour diagram depicting the cell surface densities of CD4 and CD8 in HeLa cells transfected with the null Nef mutant (NX), HIV-1, or SIV Nef are shown on the *left*. The histogram to the *right* is a plot of CD4 fluorescence in the respective transfectants gated for CD8 expression. The immunoblots on the *right* illustrate the steady-state levels of total cellular CD4 and CD8 in the transfectants. Results are representative of four experiments. *B*, Nef expression down-regulated presynthesized WT CD4 but not tCD4 at the cell surface. CD4 expression was evaluated by flow cytometry on A2D8 cell line expressing WT CD4 or a related T cell line, T402, expressing tCD4 mutant lacking the C-terminal domain. In each case, $\sim 10^6$ cells were left uninfected (UI) or infected with the control vaccinia virus, vSVC8, or the HIV-1 Nef recombinant, vvNef, at a multiplicity of infection of 10 plaque-forming units/cell as described under "Experimental Procedures." At 4 h after infection, when $>80\%$ cells were positive for vaccinia virus E3L expression, separate 10^5 cell aliquots were stained for the surface expression of CD7 and CD4 using PE or fluorescein isothiocyanate-conjugated monoclonal antibodies, respectively. Results obtained with the fluorescein isothiocyanate-conjugated CD4 antibodies are shown with the respective MFVs. The immunoblots under the FACS profile for WT CD4 represent the steady-state levels of CD4 and Nef in the respective infections or non-infections. *C* and *D*, pretreatment with NH_4Cl or chloroquine (CHQ) blocked the Nef-induced down-regulation of cell surface CD4 in A3.01 T cells (*C*) or in HeLa CD4 cells (*D*). Cells were infected with vSVC8 or vvNef at a multiplicity of infection of 10 plaque-forming units/cell and treated with NH_4Cl (75 mM for T cells and 200 mM for HeLa cells) or chloroquine (100 μM) or left untreated from 30 min after virus adsorption. Infection was continued until $>80\%$ of cells scored positively for staining with E3L antibody (typically around 4 h). Results representing two experiments are illustrated by the FACS histogram profiles of CD4 expression. CD4 MFV is denoted in each histogram.

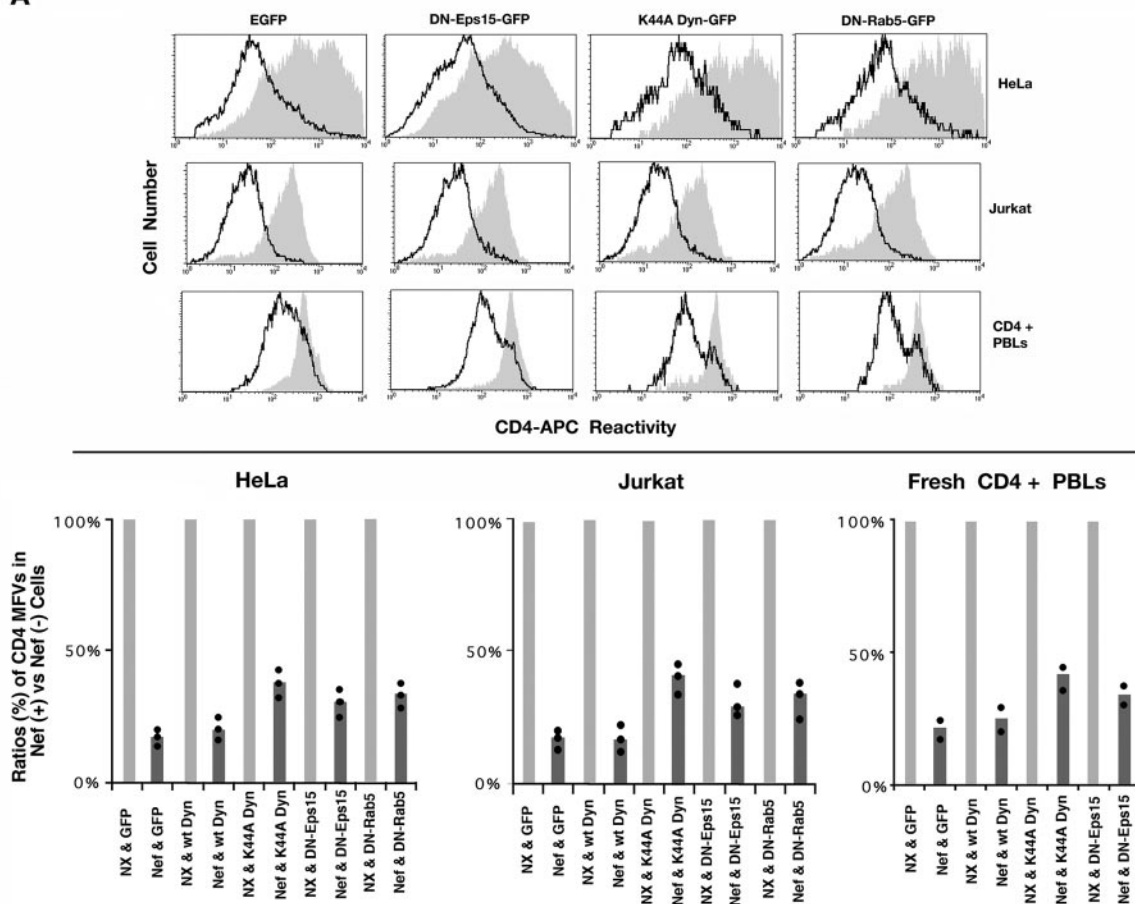
state levels of endogenous CD4 in lymphocytes and plasmid-expressed CD4 in HeLa cells. In HeLa cells, the dominant-negative inhibitors induced a slight to modest increase in the cell surface CD4 MFV, varying from a low of 133% (Eps15 mutant) to 170% (Rab5 mutant). In Jurkat T cells and PBLs, the same mutants induced little or no difference in the steady-state levels of CD4 (data not shown). Nef down-regulated the cell surface density of the endogenous and plasmid-expressed CD4 5-fold ($\pm 6\%$) in lymphocytes and epithelial cells. In a pairwise comparison of CD4 MFVs in Nef(+) versus Nef(-) HeLa cells, dominant-negative inhibitors of dynamin, Eps15, and Rab5 induced a modest reversal (44% ($\pm 6\%$), 30% ($\pm 8\%$), and 38% ($\pm 9\%$) for dynamin, Eps, and Rab5 mutants, respectively) in the magnitude of effect of Nef in both the epithelial cells and the lymphocytes (Fig. 5A).

The above results were corroborated by immunofluorescence microscopy. Steady-state distribution of CD4 was examined in HeLa cell transfectants expressing CD4, Nef, and GFP or the GFP fusion proteins described above. In the absence of functional Nef expression, CD4 was at the cell surface (Fig. 5B), whereas in the Nef-expressing cells, CD4 was predominantly distributed in perinuclear vesicles with very little at the plasma membrane (Fig. 5B, compare panels labeled NX & GFP

and Nef & GFP). This pattern was unaltered in cells expressing GFP-tagged WT dynamin. K44A dynamin, Eps15, and Rab5 dominant-negative mutants slightly increased the presence of CD4 at the plasma membrane of HIV-1 Nef-expressing cells, although the majority of CD4 was still redistributed to intracellular vesicles (Fig. 5B).

Dominant-negative Inhibitors of Endocytosis Reversed SIV Nef-induced CD4 Down-regulation—We inquired whether enhanced endocytosis (Fig. 3) constituted the principal mechanism of SIV Nef-mediated CD4 loss at the cell surface. To this end, we compared the plasma membrane CD4 levels in SIV Nef(+) versus SIV Nef(-) cells co-expressing selected dominant-negative inhibitors of endocytosis. In cells expressing GFP or GFP-tagged WT dynamin, SIV Nef induced nearly 7-fold ($\pm 12\%$) reduction in the cell surface levels of CD4 (Fig. 6B). The K44A dynamin mutant that blocks both clathrin- and non-clathrin-dependent internalization (45, 48, 49) induced 85% ($\pm 15\%$) reversal of the effect of SIV Nef on CD4. The Eps15 mutant, a specific inhibitor of clathrin-coated vesicle assembly, was inefficient in this regard. Microscopic visualization of CD4 distribution confirmed these results. Although in GFP and WT dynamin GFP-expressing SIV Nef(+) cells, CD4 was sequestered in intracellular vesicles, the receptor was pre-

A



B

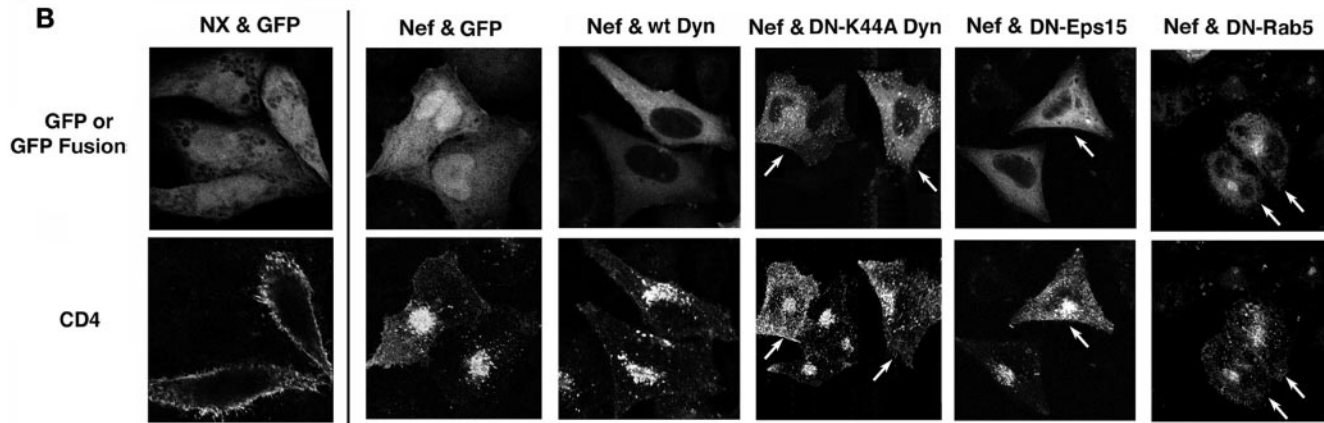


FIG. 5. Dominant-negative inhibitors of endocytosis that abrogate transferrin uptake do not significantly reverse the HIV-1 Nef-induced CD4 down-regulation. *A*, FACS histogram profiles of CD4 expression in HeLa cells, Jurkat T cells, or fresh CD4⁺ PBLs co-transfected with WT Nef or a null mutant (NX) at a 2-fold molar excess over GFP or GFP-tagged dominant-negative inhibitors of endocytosis. In HeLa cells, CD4 expression was from the co-transfected CD4 recombinant. CD4 expression profiles of NX (gray) and HIV-1 Nef (black) gated for GFP fluorescence are overlaid in each panel. CD4 MFVs of GFP (or YFP) gated populations in the NX and Nef transfectants are plotted pairwise, with the NX value in each pair arbitrarily set to 100. Results obtained in individual experiments are denoted by dots. *Dyn*, dynamin. *B*, subcellular distribution of CD4 in HeLa cells co-expressing Nef and GFP or GFP-(or YFP)-tagged effectors or inhibitors of endocytosis. HeLa cells were transfected with a 2-fold molar excess of HIV-1 Nef over CD4 and GFP or GFP/YFP fusion protein plasmids. At these ratios, Nef expression was observed in all the GFP/YFP⁺ cells (not shown). At 30 h after transfection, cells were rinsed, fixed in 4% paraformaldehyde, and permeabilized in 0.1% Triton X-100 and then stained with CD4-APC before processing for microscopy. Individual channels corresponding to GFP and CD4 fluorescence extracted from the RGB images are shown.

dominantly at the plasma membrane in cells expressing the K44A dynamin mutant (Fig. 6A). CD4 internalization dynamics in these transfectants confirmed these findings. Although both Tfn and CD4 underwent brisk internalization in cells irrespective of their GFP expression levels (Fig. 6C, left panels), endocytosis of both Tfn and CD4 was severely retarded in the K44A dynamin-expressing SIV Nef (+) cells (Fig. 6C, right,

compare the presence and absence of CD4 in the intracellular vesicles in the GFP cell versus the two K44A Dyn-GFP cells). These findings, combined with the results of Fig. 3, strongly supported the conclusion that the effect of SIV Nef on CD4 was predominantly mediated by enhanced endocytosis.

SIV but Not HIV-1 Nef-induced CD4 Down-regulation Was Reversed by siRNA-induced Depletion of AP-2—Specialized

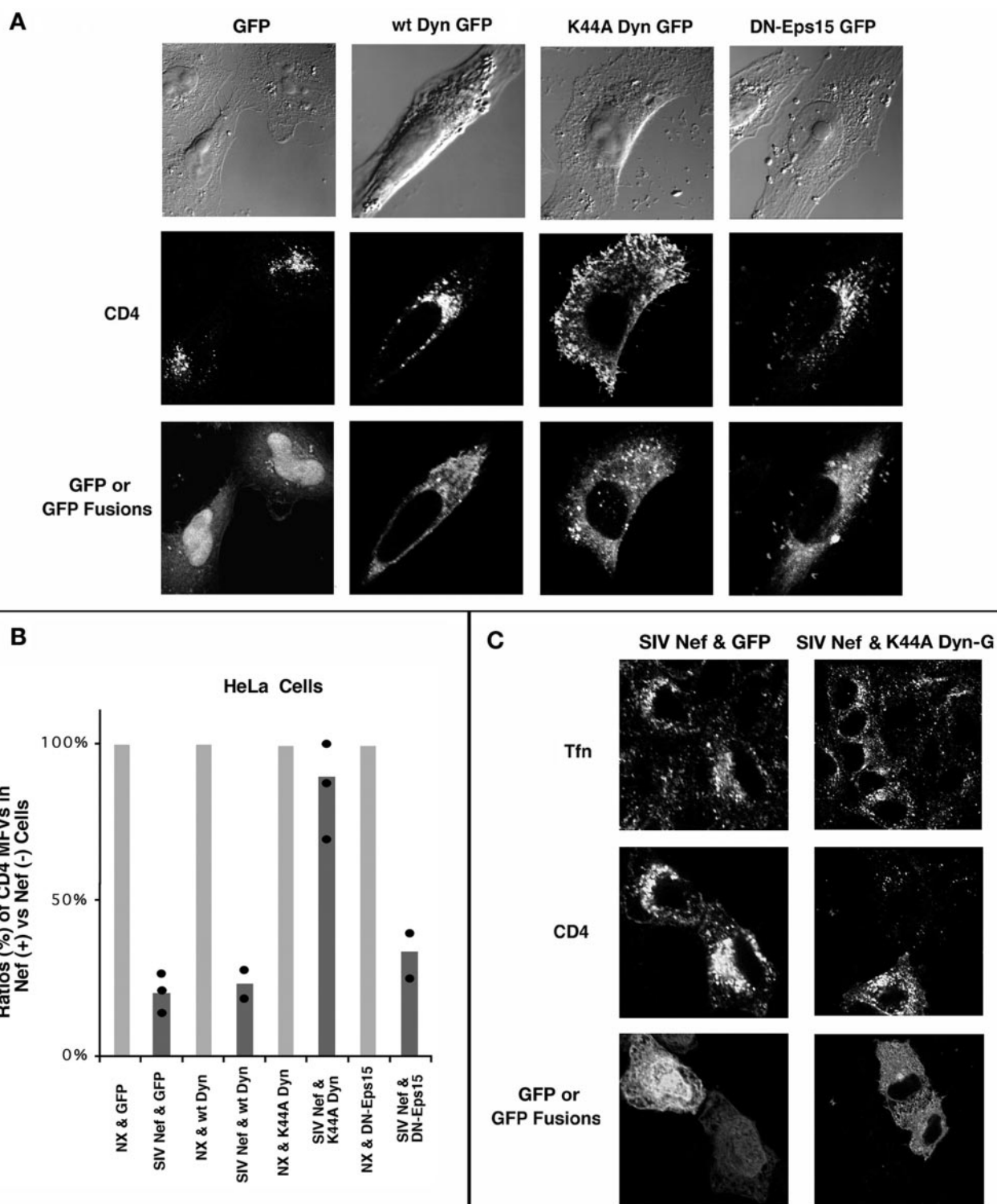
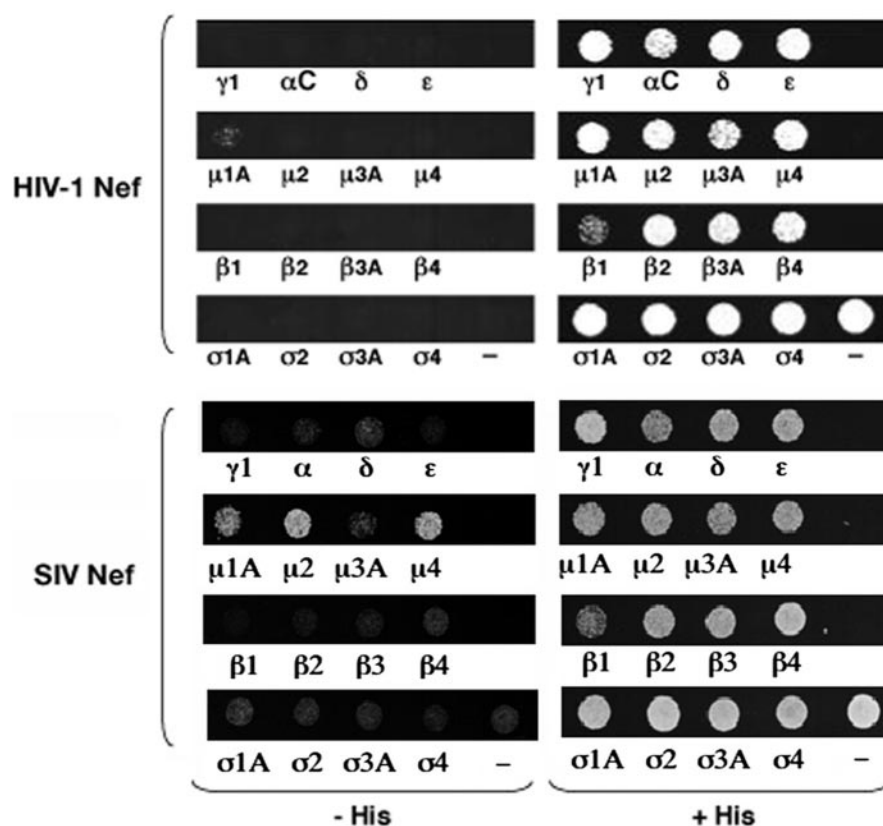


FIG. 6. Dominant-negative inhibition of endocytosis, notably by the K44A dynamin (*Dyn*) mutant, reversed the SIV Nef-mediated CD4 down-regulation. HeLa cells were transfected as in Fig. 5B except that SIV Nef was substituted for HIV-1 Nef. Identical DNA co-transfections were carried out simultaneously with 3×10^6 cells seeded on 3 wells of a 6-well plate and 10^5 cells on 8-mm glass coverslips. **A**, steady-state distribution of CD4-expressing GFP or GFP-tagged WT dynamin, the K44A dynamin, or the Eps15 Δ 95/295 mutant. RGB channels of confocal images were separated to display cell morphology, CD4 staining, and GFP or GFP-tagged fusion proteins. **B**, pairwise comparison of relative CD4 MFVs (by flow cytometry) at the plasma membrane of SIV Nef (+) versus Nef (-) (NX) cells (with the MFV in the NX cells of each pair arbitrarily set to 100) expressing GFP or GFP-tagged proteins. **C**, Tfn uptake and active CD4 endocytosis visualized simultaneously in cells expressing SIV Nef and GFP or GFP-tagged K44A dynamin mutant. CD4 endocytosis was measured by feeding transfectants APC-conjugated mAb and Texas-Red labeled Tfn as described under "Experimental Procedures." Cell surface-bound mAb and Tfn were stripped by acid wash before mounting. An RGB image of each field was separated into individual channels corresponding to GFP or GFP fusion protein, CD4, and Tfn.

protein-coated vesicles mediate the sorting of transmembrane proteins during antero- and retrograde trafficking between the Golgi, trans-Golgi network, plasma membrane, endosomes,

and lysosomes. There are four major heterotetrameric coat protein complexes, referred to as adaptors AP-1, AP-2, AP-3, and AP-4, which are composed respectively of two large (one

FIG. 7. SIV Nef bound $\mu 2$, and to a lesser extent $\mu 1a$ and $\mu 4$ adaptor subunits of adaptor complexes, whereas HIV-1 Nef bound weakly and only to the $\mu 1a$ subunit. Two-hybrid analysis of interaction between full-length HIV-1 or SIV Nef with the different AP subunits (expressed from pGADT7 or pGAD424) as described elsewhere (15) is shown. Yeast cells were co-transformed with plasmids encoding the combination of constructs shown in the figure. Interactions were evidenced by growth on agar plates made with medium without histidine ($-His$).



each of $\gamma/\alpha/\delta/\epsilon$ and $\beta 1-4$), one medium ($\mu 1-4$), and one small ($\sigma 1-4$) protein chain. Intracellular trafficking of membrane proteins is governed by specific interactions between signals in the cytoplasmic domain of membrane proteins with the adaptor protein components (1-3, 50). Two tyrosine motifs at the N-terminal region of SIV Nef that mediate its binding to the AP-2 complex, presumably via the $\mu 2$ subunit, have been shown to be critical for SIV Nef-induced CD4 down-regulation (17, 18). Consistent with these observations, SIV Nef bound $\mu 2$, and to a lesser extent, $\mu 1a$ and $\mu 4$ adaptor subunits in the yeast 2-hybrid assay. Under the same conditions, HIV-1 Nef bound only the $\mu 1a$ subunit weakly (Fig. 7). On the basis of this finding, we inquired whether the effect of SIV Nef on CD4 could be reversed by siRNA-induced knockdown of AP-2 complexes. Treatment of HeLa cells with siRNA against the $\mu 2$ chain mRNA induced a marked depletion of AP-2 complexes as shown by immunofluorescence using antibody against α -adaptin. $\mu 2$ siRNA had no effect on the distribution of AP-1 or AP-3 complexes (Fig. 8A). Loss of AP-2 complexes induced by $\mu 2$ siRNA treatment was correlated with impaired clathrin-mediated endocytosis, demonstrated by the marked inhibition of transferrin uptake (Fig. 8B). $\mu 2$ siRNA treatment also increased the steady-state levels TfnR (CD71) 8-fold ($\pm 20\%$), which reflected the strong inhibition of constitutive endocytosis of TfnR (Fig. 8B, bottom). AP-2 depletion in HeLa cells resulted in a dramatic reversal ($90\% \pm 15\%$) of the effect of SIV Nef on CD4 expression (Fig. 8C, left panel). AP-2 depletion did not rectify the residual ($\sim 50\%$ of WT) effect on CD4 of SIV Nef Y28A mutant, lacking the $\mu 2$ binding potential. In contrast to SIV Nef, the effect of HIV-1 Nef on CD4 was only slightly ($25\% \pm 7\%$) reversed by $\mu 2$ (Fig. 8C, right panel) knockdown. These results conclusively demonstrated that $\mu 2$ depletion and the resulting decrease in the AP-2-dependent endocytosis impaired SIV Nef but not HIV-1 Nef-induced CD4 down-regulation.

DISCUSSION

Through multiple lines of evidence, we have shown that CD4 down-regulation by HIV-1 and SIV Nef proteins involves both internalization and intracellular retention mechanisms to different extents. SIV Nef predominantly enhanced endocytosis in an AP-2-dependent pathway. HIV-1 (NL4-3 strain) Nef, which binds to AP-1 and AP-3 hemicomplexes, but not AP-2 complex or subunits (15), down-regulated CD4 by promoting intracellular retention of recycling and/or nascent CD4 and probable rerouting of the receptor to the lysosomes.

Many studies have underscored enhanced endocytosis as the *prima facie* mechanism of Nef-induced CD4 down-regulation and correlated this mechanism with the physical interaction of Nef with the subunits of AP-1 or AP-2 adaptor complexes (10, 11, 16-18, 51-53). We have shown that the few HIV-1 Nef alleles we tested interacted weakly, if at all, with the $\mu 2$ subunit alone or in combination with the other adaptor subunits. However, we reported before that many different HIV-1 Nef alleles interacted with preformed $\gamma\sigma 1$ and $\delta\sigma 3$ hemicomplexes of AP-1 and AP-3 adaptors via a (D/E)XXXL(L/I) sequence in the unstructured C-terminal loop of Nef (15). As predicted from the lack of AP-2 binding, HIV-1 Nef did not significantly augment CD4 endocytic rate in HeLa cells. AP-1 and AP-3 regulate vesicular traffic of proteins between trans-Golgi network, endosomes, and plasma membrane, and as expected from such interactions, HIV-1 Nef reduced the recycling rate of internalized CD4 2-3-fold.

SIV Nef, which has both a canonical YXX Φ sequence near the N terminus and a EEHYLMHPA sequence (where the -LM-dipeptide is highlighted in bold and the dileucine motif equivalent is underlined) near the C terminus, binds to the AP-2 adaptor (11, 17, 38), via the $\mu 2$ subunit (Ref. 18 and this study) and the $\gamma\sigma 1$ AP-1 hemi-complex (15), respectively. Consistent with these properties, SIV Nef significantly enhanced the constitutive internalization of CD4 in HeLa cells. However,

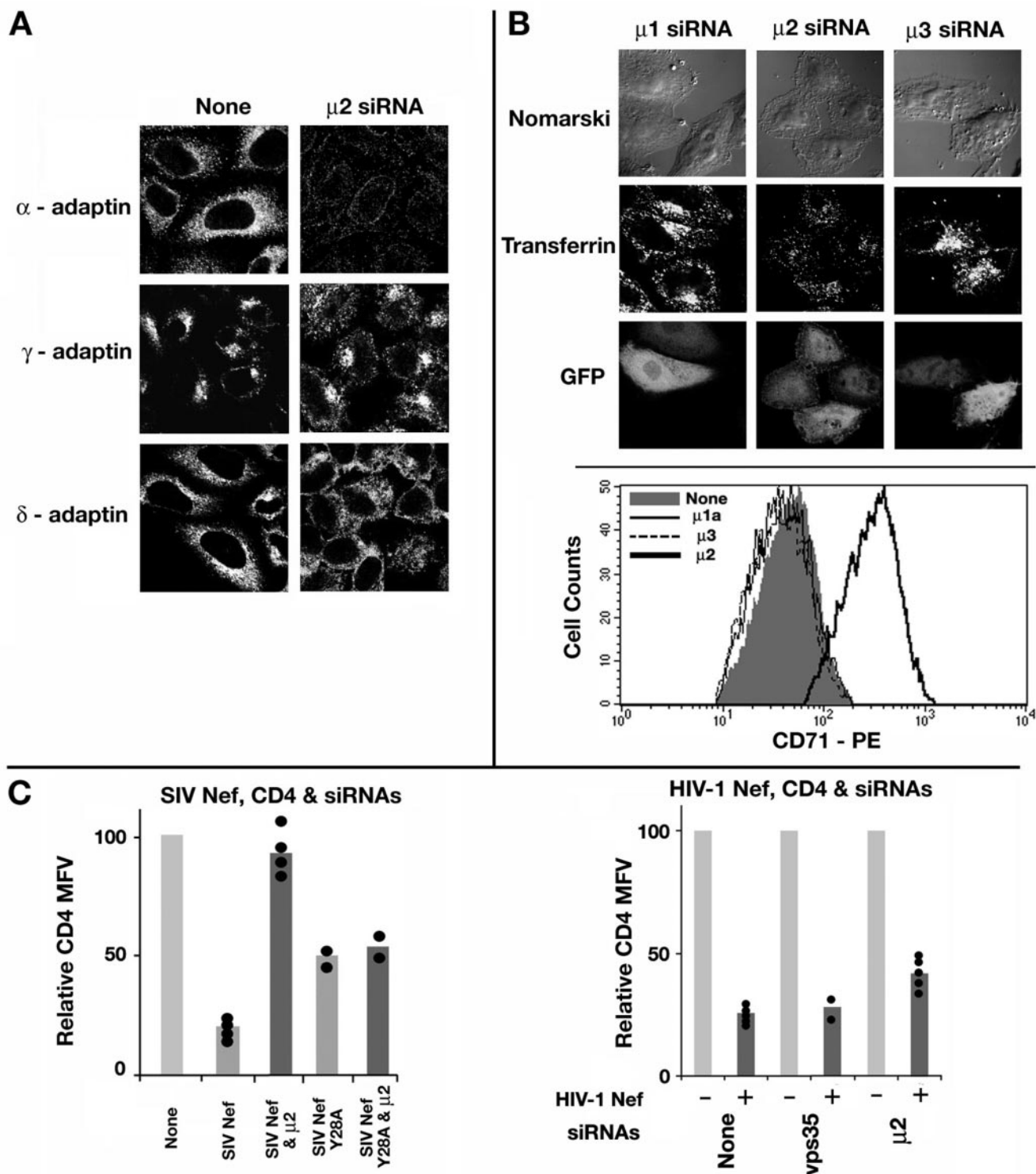


FIG. 8. AP-2 depletion had a significantly better corrective effect on SIV Nef than HIV-1 Nef-induced CD4 down-regulation. A, siRNA against $\mu 2$ knocks down AP-2 vesicle assembly but not other related adaptor vesicles. Mock- or $\mu 1A$ siRNA-transfected HeLa cells were analyzed by immunofluorescence microscopy with antibodies against α , $\gamma 1$, or δ adaptor subunits. B, $\mu 2$ but not $\mu 1a$ or $\mu 3$ siRNA expression reduced transferrin uptake (top) and the steady-state levels of transferrin receptor (CD71). Mock- or siRNA-treated cells were transfected with plasmids for CD4 and GFP and with a 2-fold excess of various WT, mutant Nef, or null expression plasmids. Aliquots of various HeLa cell transfectants were plated on coverslips and analyzed for transferrin uptake by confocal microscopy as described before. The histogram plots below represent relative CD71 MFVs in the different siRNA-treated cells. C, histogram plots of relative CD4 MFVs in HeLa cells pretreated with the indicated siRNAs or left untreated prior to co-transfection with CD4, GFP, and the respective Nef derivatives. For each siRNA-treated batch, CD4 MFVs of GFP gated populations in the NX and Nef transfectants are plotted pairwise, with the NX value in each pair set to 100. Results from HeLa cells treated with siRNAs against $\mu 2$, vps35, or untreated prior to transfection with CD4, GFP and a 2-fold excess of HIV-1 Nef or null (NX) plasmids are shown on the left. Results with WT or mutant SIV Nef or empty vector plasmids are on the right.

SIV Nef did not augment the internalization of the LL/AA CD4 mutant that lacked the AP-2 binding potential and was therefore not endocytosed constitutively (13). Since SIV Nef binds

AP-2 and probably CD4, these findings implied that SIV Nef reinforced weak CD4/AP-2 interactions.

It was of interest that both HIV-1 and SIV Nef enhanced

CD4 internalization in Jurkat lymphocytes, wherein tethering of CD4 to the tyrosine kinase, *p56 lck*, inhibits constitutive receptor recycling (43, 44). Both Nef proteins would be expected to dissociate *p56 lck* from CD4 in T cells (54) and thus allow constitutive CD4 internalization (13, 43). The temporal lag in CD4 endocytosis in HIV-1 Nef cells probably reflected this process. The faster CD4 endocytic kinetics in the SIV Nef cells reflects the combination of enhanced AP-2 recruitment and CD4 dissociation from *p56 lck*.

Genetic perturbation of endocytic trafficking elucidated the relative importance of CD4 endocytosis in the receptor down-modulation by HIV-1 versus SIV Nef. Inhibition of clathrin-coated vesicle assembly by the Eps15 Δ 95/295 mutant or endosomal traffic by the Rab5-S34N mutant induced a modest reversal of HIV-1 Nef-induced CD4 loss. However, the K44A dynamin mutant, an inhibitor of both clathrin-dependent and clathrin-independent endocytosis, was much better than the other inhibitors in partially rectifying the HIV-1 Nef effect. Microscopic analysis of CD4 distribution in cells expressing HIV-1 Nef and the various dominant-negative mutants corroborated the FACS analysis. In contrast, the effect of SIV Nef on CD4 was almost completely reversed by the K44A dynamin mutant in both the FACS and the microscopic assay. The Eps15 Δ 95/295 mutant was, however, much less efficient in this regard.

siRNA-driven AP-2 knockdown almost completely reversed the SIV Nef-induced CD4 down-regulation, thus corroborating the results observed with the dominant-negative inhibitors of endocytosis. Disruption of AP-2 vesicles by μ 2-specific siRNA treatment did not cause a comparable reversal of HIV-1 Nef effect on CD4. The SIV Nef Y28A mutant, lacking the AP-2 binding potential, had a residual effect on CD4 that was also resistant to μ 2 knockdown. An earlier report (17) suggested that SIV Nef employed both the dileucine and tyrosine motifs to promote CD4 internalization. However, our results suggest that tyrosine motif-based AP-2 sorting is the predominant mechanism for the WT SIV Nef, and the dileucine motif may be only operative when the tyrosine motif is mutated.

The ultimate test for the involvement of AP-1 in Nef-induced CD4 down-regulation *in vivo* would be to examine the effect of AP-1 depletion on this process. However, siRNA-induced knockdown of AP-1 vesicles was incomplete and did not consistently rectify the HIV-1 Nef-induced CD4 down-regulation. The fact that the inhibition of HIV-1 Nef effect was incomplete could be due to the small residual levels of AP-1 in the treated cells, usage of alternative isoforms of AP-1 subunits, the low threshold of AP-1 for the Nef effect, or the secondary contribution of AP-3 or other proteins to CD4 down-regulation.

There was substantial intracellular retention of CD4 in transport vesicles in HIV-1 Nef transfectants, which might represent internalized receptor stalled during recycling and/or nascent receptor *en route* to the plasma membrane. Using recombinant vaccinia viruses to simultaneously express CD4 and Nef in CD4-negative T cells, we showed that Nef markedly delayed the cell surface presentation of *de novo* CD4 and reduced its plasma membrane density 3-fold. It was unlikely that the delay (obvious within 1 h after infection) in the appearance of *de novo* synthesized CD4 at the plasma membrane of Nef(+) cells resulted from enhanced endocytosis. More direct proof for an anterograde transport defect was obtained in pulse-chase labeling of recombinant vaccinia virus-infected cells. Nef induced a rapid turnover of nascent CD4 within 1–2 h of the metabolic chase. This defect was specific for CD4 with a cytoplasmic tail; truncated CD4 lacking the cytoplasmic domain and unrelated cellular and viral surface glycoproteins (such as CD46 and HIV-1 *env* gp160 and influenza virus HA (not shown)

were unaffected by Nef. CD4 turnover rates were also markedly enhanced in epithelial cells with a $t_{1/2}$ as brief as 30 min. Consistent with the previous reports (55, 56), Nef did not alter the rate or the magnitude of CD4 maturation in the Golgi when analyzed by acquisition of endoglycosidase H resistance (data not shown). Since endocytic degradation alone could not account for the short $t_{1/2}$ (as long as the labeling time) of CD4 turnover in Nef-expressing cells, our findings implied that HIV-1 Nef was inducing intracellular retention of CD4 during the post-Golgi itinerary. An earlier report suggested that interaction of a diacidic motif of HIV-1 Nef with the β subunit of COPI coatamers targeted the internalized CD4 for endosomal degradation (57). However, a later report has shown that this diacidic motif was irrelevant for the effect of Nef on CD4 (58), and we have conclusively demonstrated the primacy of the dileucine motif for HIV-1 Nef-induced CD4 down-regulation (15).

Notwithstanding the above results showing intracellular retention of concurrently synthesized CD4, Nef also induced aberrant recycling and intracellular degradation of plasma membrane-associated receptor. Using a vaccinia expression system, we demonstrated that Nef reduced the cell surface levels of presynthesized endogenous CD4 in both lymphocytes and epithelial cells. Since vaccinia virus shuts off host cell protein synthesis within a few minutes after virus entry, it is reasonable to conclude that the loss of cell surface CD4 resulted from aberrant endocytic recycling and lysosomal degradation of the receptor. Consistent with this scenario, treatment of cells with lysosomotropic agents such as NH_4Cl or chloroquine almost completely inhibited the receptor loss induced by Nef. Although HIV-1 or SIV Nef moderately reduced the steady-state levels of CD4 during transient co-expression (Fig. 4A), it was not possible to rectify the total CD4 loss for the following reasons. 1) Typically, steady-state CD4 was examined at 24–48 h after in transfections, which was far longer than the limited duration (\sim 4 h) that the cells could be exposed to lysosomotropic agents without causing cytotoxicity. 2) It was not possible to discriminate in metabolic labeling experiments the effects of HIV-1 Nef on *de novo* synthesized CD4 in transit to or recycling from the plasma membrane since the Nef effects were obvious even at 20 min during the chase (Fig. 1B and 2). 3) Arresting protein synthesis with cycloheximide after brief labeling was not feasible since Nef turned over more rapidly with a $t_{1/2}$ of \sim 1 h (not shown) than CD4 with a $t_{1/2}$ of about 6 h in Nef(+) and 12–18 h in Nef(–) cells. Nevertheless, it is worthwhile to highlight the different *modus operandi* of HIV-1 versus SIV Nef. SIV-1 Nef was much more potent than HIV-1 Nef in enhancing CD4 endocytosis in Jurkat T lymphocytes, and siRNA-mediated ablation of AP-2 vesicles was more efficient in reversing the SIV Nef effect. Therefore, the dominant effect of HIV-1 Nef on CD4 at the cell surface reflects aberrant recycling rather than enhanced endocytosis. Whether internalized by enhanced endocytosis or trapped intracellularly by retarded recycling, CD4 is degraded in the lysosomes.

In summary, our studies have shown that AP-2-mediated enhanced CD4 endocytosis is the predominant (if not the exclusive) mechanism used by SIV Nef, which has a canonical tyrosine motif near the N terminus that binds to the AP-2 μ 2 subunit. HIV-1 (NL4-3) Nef, which lacks the tyrosine motif and the μ 2 binding potential, enhanced CD4 endocytosis only slightly. These conclusions must be tempered by the reality that our results for SIV Nef were obtained with human CD4 in human cells. Whether SIV Nef has evolved different strategies for interacting with non-human primate CD4 and/or adaptor complexes remains to be tested.

Physical interaction of HIV-1 Nef and CD4 has been demon-

strated in insect cells overexpressing both proteins (19), in yeast two-hybrid system (20) and *in vitro* binding assays using purified Nef protein and CD4 cytoplasmic domain peptides (21, 59). *In vitro* binding of Nef to a CD4 C-tail peptide occurs via a hydrophobic patch on Nef including Trp-57, Leu-58, and Leu-110 residues and requires 2 leucines in the CD4 peptide (21). However, stable complexes of HIV-1 Nef and LL/AA CD4 mutant have been demonstrated in mammalian cells, suggesting that the dileucine motif of CD4 may not be critical for Nef binding (60). The dileucine motif in the C-tail of CD4 was shown to interact with the AP-1 complex (61, 62), albeit weakly and requiring phosphorylation at a proximal or a distal serine residue (13). Both HIV-1 and SIV Nef have a dileucine motif and trap both the nascent CD4 *en route* to plasma membrane and the internalized CD4 during recycling, presumably through a tripartite recognition between the (D/E)XXXL(L/I) signal in Nef and the C-tail of CD4 with the two subunits of the AP-1 and AP-3 complexes, $\gamma 1\text{-}\sigma 1$ and $\delta\text{-}\sigma 3$, respectively (15).

Of the 10 different HIV-1 Nef alleles that we have tested for their effect on CD4, only NA-7 has both the canonical YXX Φ tyrosine motif near the N terminus and an -LL- motif at position 164. Although we have not tested NA-7 Nef for its binding potential to the AP-2 $\mu 2$ subunit, siRNA-induced AP-2 knock-down failed to reverse the NA-7-induced CD4 down-modulation (data not shown). Although most SIV Nef alleles have both tyrosine and dileucine motifs, Nef encoded by the chimpanzee SIV-cpz (which is closely related to HIV-1) does not. Thus, it appears that HIV Nef proteins have evolved preferential usage of dileucine-based sorting mechanisms.

Acknowledgments—We thank S. Popov for help in purifying recombinant vaccinia viruses and for some preliminary experiments. We thank Sophie Gratton of Universite de Montreal, Montreal, Quebec, Canada for help and discussions relating to FACS analysis of vaccinia virus-infected cells. Recombinant vaccinia viruses expressing WT or tCD4, gp 160, or CD46 were obtained from Patricia Earl, Laboratory of Viral Diseases, NIAID, National Institutes of Health, or Chris Broder of Uniformed Services University of the Health Sciences, Bethesda, MD. We thank Robert Lodge at the INRS-Institut Armand-Frappier, Université du Québec, Laval, Québec, Canada for mutant Rab plasmids and Jacek Skowronski of Cold Spring Harbor Laboratories, Cold Spring Harbor, NY for the pCG-SIV Nef plasmid.

REFERENCES

1. Bonifacino, J. S., and Traub, L. M. (2003) *Annu. Rev. Biochem.* **72**, 395–447
2. Mellman, I. (1996) *Annu. Rev. Cell Dev. Biol.* **12**, 575–625
3. Robinson, M. S., and Bonifacino, J. S. (2001) *Curr. Opin. Cell Biol.* **13**, 444–453
4. Geyer, M., Fackler, O. T., and Peterlin, B. M. (2001) *EMBO Rep.* **2**, 580–585
5. Wei, B. L., Arora, V. K., Foster, J. L., Sodora, D. L., and Garcia, J. V. (2003) *Curr. HIV Res.* **1**, 41–50
6. Oldridge, J., and Marsh, M. (1998) *Trends Cell Biol.* **8**, 302–305
7. Piguet, V., Wan, L., Borel, C., Mangasarian, A., Demaurex, N., Thomas, G., and Trono, D. (2000) *Nat. Cell Biol.* **2**, 163–167
8. Mangasarian, A., Piguet, V., Wang, J. K., Chen, Y. L., and Trono, D. (1999) *J. Virol.* **73**, 1964–1973
9. Greenberg, M. E., Iafrate, A. J., and Skowronski, J. (1998) *EMBO J.* **17**, 2777–2789
10. Craig, H. M., Pandori, M. W., and Guatelli, J. C. (1998) *Proc. Natl. Acad. Sci. U. S. A.* **95**, 11229–11234
11. Bresnahan, P. A., Yonemoto, W., Ferrell, S., Williams-Herman, D., Geleziunas, R., and Greene, W. C. (1998) *Curr. Biol.* **8**, 1235–1238
12. Aiken, C., Konner, J., Landau, N. R., Lenburg, M. E., and Trono, D. (1994) *Cell* **76**, 853–864
13. Pitcher, C., Honing, S., Fingerhut, A., Bowers, K., and Marsh, M. (1999) *Mol. Biol. Cell* **10**, 677–691
14. Greenberg, M., DeTulleo, L., Rapoport, I., Skowronski, J., and Kirchhausen, T. (1998) *Curr. Biol.* **8**, 1239–1242
15. Janvier, K., Kato, Y., Boehm, M., Rose, J. R., Martina, J. A., Kim, B. Y., Venkatesan, S., and Bonifacino, J. S. (2003) *J. Cell Biol.* **163**, 1281–1290
16. Mangasarian, A., Foti, M., Aiken, C., Chin, D., Carpentier, J. L., and Trono, D. (1997) *Immunity* **6**, 67–77

17. Bresnahan, P. A., Yonemoto, W., and Greene, W. C. (1999) *J. Immunol.* **163**, 2977–2981
18. Piguet, V., Chen, Y. L., Mangasarian, A., Foti, M., Carpentier, J. L., and Trono, D. (1998) *EMBO J.* **17**, 2472–2481
19. Harris, M. P., and Neil, J. C. (1994) *J. Mol. Biol.* **241**, 136–142
20. Rossi, F., Gallina, A., and Milanesi, G. (1996) *Virology* **217**, 397–403
21. Grzesiek, S., Stahl, S. J., Wingfield, P. T., and Bax, A. (1996) *Biochemistry* **35**, 10256–10261
22. Preusser, A., Briese, L., Baur, A. S., and Willbold, D. (2001) *J. Virol.* **75**, 3960–3964
23. Gratton, S., Yao, X. J., Venkatesan, S., Cohen, E. A., and Sekaly, R. P. (1996) *J. Immunol.* **157**, 3305–3311
24. Venkatesan, S., Rose, J. J., Lodge, R., Murphy, P. M., and Foley, J. F. (2003) *Mol. Biol. Cell* **14**, 3305–3324
25. Chakrabarti, S., Brechling, K., and Moss, B. (1985) *Mol. Cell. Biol.* **5**, 3403–3409
26. Koenig, S., Fuerst, T. R., Wood, L. V., Woods, R. M., Suzich, J. A., Jones, G. M., de la Cruz, V. F., Davey, R. J., Venkatesan, S., Moss, B., Biddeson, W. E., and Fauci, A. S. (1990) *J. Immunol.* **145**, 127–135
27. Broder, C. C., and Berger, E. A. (1993) *J. Virol.* **67**, 913–926
28. Golding, H., Dimitrov, D. S., Manischewitz, J., Broder, C. C., Robinson, J., Fabian, S., Littman, D. R., and Lapham, C. K. (1995) *J. Virol.* **69**, 6140–6148
29. Earl, P. L., Hugin, A. W., and Moss, B. (1990) *J. Virol.* **64**, 2448–2451
30. Earl, P. L., Doms, R. W., and Moss, B. (1990) *Proc. Natl. Acad. Sci. U. S. A.* **87**, 648–652
31. Nussbaum, O., Broder, C. C., Moss, B., Stern, L. B.-L., Rozenblatt, S., and Berger, E. A. (1995) *J. Virol.* **69**, 3341–3349
32. Maitra, R. K., Ahmad, N., Holland, S. M., and Venkatesan, S. (1991) *Virology* **182**, 522–533
33. Venkatesan, S., Gerstberger, S. M., Park, H., Holland, S. M., and Nam, Y. (1992) *J. Virol.* **66**, 7469–7480
34. Benmerah, A., Bayrou, M., Cerf-Bensussan, N., and Dautry-Varsat, A. (1999) *J. Cell Sci.* **112**, 1303–1311
35. Damke, H., Baba, T., Warnock, D. E., and Schmid, S. L. (1994) *J. Cell Biol.* **127**, 915–934
36. Dell'Angelica, E. C., Ooi, C. E., and Bonifacino, J. S. (1997) *J. Biol. Chem.* **272**, 15078–15084
37. Yuwen, H., Cox, J. H., Yewdell, J., Bannick, J. R., and Moss, B. (1993) *Virology* **195**, 732–744
38. Greenberg, M. E., Bronson, S., Lock, M., Neumann, M., Pavlakis, G. N., and Skowronski, J. (1997) *EMBO J.* **16**, 6964–6976
39. Pelchen-Matthews, A., Armes, J. E., and Marsh, M. (1989) *EMBO J.* **8**, 3641–3649
40. Bour, S., Boulerice, F., and Wainberg, M. A. (1991) *J. Virol.* **65**, 6387–6396
41. Willey, R. L., Maldarelli, F., Martin, M. A., and Strebel, K. (1992) *J. Virol.* **66**, 7193–7200
42. Willey, R. L., Maldarelli, F., Martin, M. A., and Strebel, K. (1992) *J. Virol.* **66**, 226–234
43. Pelchen-Matthews, A., Boulet, I., Littman, D. R., Fagard, R., and Marsh, M. (1992) *J. Cell Biol.* **117**, 279–290
44. Pelchen-Matthews, A., Armes, J. E., Griffiths, G., and Marsh, M. (1991) *J. Exp. Med.* **173**, 575–587
45. Schmid, S. L., McNiven, M. A., and De Camilli, P. (1998) *Curr. Opin. Cell Biol.* **10**, 504–512
46. Chen, H., Fre, S., Slepnev, V. I., Capua, M. R., Takei, K., Butler, M. H., Di Fiore, P. P., and De Camilli, P. (1998) *Nature* **394**, 793–797
47. Somsel Rodman, J., and Wandering-Ness, A. (2000) *J. Cell Sci.* **113**, 183–192
48. McNiven, M. A., Cao, H., Pitts, K. R., and Yoon, Y. (2000) *Trends Biochem. Sci.* **25**, 115–120
49. Nabi, I. R., and Le, P. U. (2003) *J. Cell Biol.* **161**, 673–677
50. Boehm, M., and Bonifacino, J. S. (2002) *Gene* **286**, 175–186
51. Craig, H. M., Reddy, T. R., Riggs, N. L., Dao, P. P., and Guatelli, J. C. (2000) *Virology* **271**, 9–17
52. Foti, M., Mangasarian, A., Piguet, V., Lew, D. P., Krause, K. H., Trono, D., and Carpentier, J. L. (1997) *J. Cell Biol.* **139**, 37–47
53. Lock, M., Greenberg, M. E., Iafrate, A. J., Swigut, T., Muench, J., Kirchhoff, F., Shohdy, N., and Skowronski, J. (1999) *EMBO J.* **18**, 2722–2733
54. Kim, Y. H., Chang, S. H., Kwon, J. H., and Rhee, S. S. (1999) *Virology* **257**, 208–219
55. Rhee, S. S., and Marsh, J. W. (1994) *J. Virol.* **68**, 5156–5163
56. Benson, R. E., Sanfridson, A., Ottinger, J. S., Doyle, C., and Cullen, B. R. (1993) *J. Exp. Med.* **177**, 1561–1566
57. Piguet, V., Gu, F., Foti, M., Demaurex, N., Gruenberg, J., Carpentier, J. L., and Trono, D. (1999) *Cell* **97**, 63–73
58. Janvier, K., Craig, H., Le Gall, S., Benarous, R., Guatelli, J., Schwartz, O., and Benichou, S. (2001) *J. Virol.* **75**, 3971–3976
59. Preusser, A., Briese, L., and Willbold, D. (2002) *Biochem. Biophys. Res. Commun.* **292**, 734–740
60. Bentham, M., Mazaleyrat, S., and Harris, M. (2003) *J. Gen. Virol.* **84**, 2705–2713
61. Rapoport, I., Chen, Y. C., Cupers, P., Shoelson, S. E., and Kirchhausen, T. (1998) *EMBO J.* **17**, 2148–2155
62. Dietrich, J., Kastrop, J., Nielsen, B. L., Odum, N., and Geisler, C. (1997) *J. Cell Biol.* **138**, 271–281